THE JOURNAL OF BIOLOGICAL CHEMISTRY VOL. 285, NO. 13, pp. 10078–10086, March 26, 2010

Stefin B Interacts with Histones and Cathepsin L in the Nucleus*

Received for publication, June 17, 2009, and in revised form, January 8, 2010 Published, JBC Papers in Press, January 14, 2010, DOI 10.1074/jbc.M109.034793

Slavko Čeru[‡], Špela Konjar[‡], Katarina Maher[‡], Urška Repnik[‡], Igor Križaj[§], Mojca Benčina[¶], Miha Renko[‡], Alain Nepveu[‖], Eva Žerovnik[‡], Boris Turk[‡], and Nataša Kopitar-Jerala[‡1]

From the Departments of [‡]Biochemistry and Molecular and Structural Biology and [§]Molecular and Biomedical Sciences, Jožef Stefan Institute, Ljubljana SI-1000, Slovenia, the [¶]Department of Biotechnology, National Institute of Chemistry, Ljubljana SI-1000, Slovenia, and the [‖]Molecular Oncology Group, McGill University, Montreal, Quebec H3A 1A1, Canada

Stefin B (cystatin B) is an endogenous inhibitor of cysteine proteinases localized in the nucleus and the cytosol. Loss-of-function mutations in the stefin B gene (*CSTB*) gene were reported in patients with Unverricht-Lundborg disease (EPM1). We have identified an interaction between stefin B and nucleosomes, specifically with histones H2A.Z, H2B, and H3. In synchronized T98G cells, stefin B co-immunoprecipitated with histone H3, predominantly in the G_1 phase of the cell cycle. Stefin B-deficient mouse embryonic fibroblasts entered S phase earlier than wild type mouse embryonic fibroblasts. In contrast, increased expression of stefin B in the nucleus delayed cell cycle progression in T98G cells. The delay in cell cycle progression was associated with the inhibition of cathepsin L in the nucleus, as judged from the decreased cleavage of the CUX1 transcription factor. *In vitro*, inhibition of cathepsin L by stefin B was potentiated in the presence of histones, whereas histones alone did not affect the cathepsin L activity. Interaction of stefin B with the Met-75 truncated form of cathepsin L in the nucleus was confirmed by fluorescence resonance energy transfer experiments in the living cells. Stefin B could thus play an important role in regulating the proteolytic activity of cathepsin L in the nucleus, protecting substrates such as transcription factors from its proteolytic processing.

Cysteine cathepsins are involved in protein degradation (1) and the development and function of the immune system (2). Cathepsin L is an endopeptidase that is able to perform limited proteolysis in the endosomes and lysosomes of specific cell types. Besides its role in hair formation and skin metabolism, it is involved in T-cell selection and NKT cell development (3). It participates in processing the major histocompatibility complex II invariant chain in thymic cortex epithelial cells (4), encephalin in chromaffin granules of neuroendocrine cells (5), and in the degradation and recycling of growth factors and their receptors in epidermal keratinocytes (6). Cathepsin L is also associated with an endosomal processing step during invasion of cells by Ebola virus (7), severe acute respiratory syndrome (SARS) coronavirus (8), and murine hepatitis coronavirus (9). As the result of gene duplication, the human genome encodes for two cathepsin L-like proteases, namely the human cathepsin L and cathepsin V (cathepsin L2), whereas in mouse only cathepsin L is present (10). At the protein level, mouse cathepsin L displays a higher sequence homology to human cathepsin V than to human cathepsin L (11). Cathepsin V shares 80% protein sequence identity with cathepsin L, but in contrast to the ubiquitously expressed cathepsin L, its expression is restricted to thymus and testis (11, 12).

Recently, the otherwise endosomal proteinase cathepsin L has been reported to be active in the nucleus. It cleaves the CUX1 transcription factor and as a result accelerates progression into the S phase of the cell cycle (13). Cathepsin L deficiency was shown to cause a global rearrangement of chromatin structure and redistribution of specifically modified histones (14). In addition, cathepsin L was found to cleave histone H3.2 in the nucleus during mouse embryonic stem cell differentiation (15).

Cathepsin L is inhibited *in vitro* by a number of proteins as follows: cystatins (16), thyropins (17), and some of the serpins (18, 19). Type 1 cystatins, or stefins, are mainly intracellular, whereas type 2 cystatins are predominantly secreted (20, 21). Stefin B is localized in the cytosol and nucleus of proliferating cells (22). Loss-of-function mutations in the cystatin B (*CTSB*, *stefin B*) gene are found in patients with Unverricht-Lundborg disease (EPM1), but its physiological implication in the pathogenesis of the disease has yet to be defined (23–26). EPM1 is an autosomal recessive inherited disease in which patients suffer from myoclonic jerks, tonic-clonic epileptic seizures, and progressive decline in cognition (26). Histopathological examination of the brain has shown neural degeneration in several areas of the central nervous system, with cerebellar damage and serious alterations of Purkinje cells (27). The most common mutation in EPM1 patients is a dodecamer repeat expansion in the stefin B (*CSTB*) gene promoter region that leads to reduced mRNA and protein levels (23, 25). In addition, four mutations in the coding region were reported in EPM1 (23, 28).

Not only cystatins but also some other proteinase inhibitors are found in the nucleus. A serine proteinase inhibitor (serpin), the myeloid and erythroid nuclear termination stage-specific protein, MENT,[2] was the first described cysteine proteinase inhibitor that interacts with chromatin and influences heterochromatin distribution (29, 30).

* This work was supported by Slovenian Research Agency Grants J3-9324 and J3-0612 (to N. K. J.) and Grant P-0140 (to V. T. and B. T.).

[1] To whom correspondence should be addressed. Tel.: 386-1-477-3510; Fax: 386-1-477-3984; E-mail: natasa.kopitar@ijs.si.

[2] The abbreviations used are: MENT, myeloid and erythroid nuclear termination stage-specific protein; E-64d, L-*trans*-epoxysuccinyl(OEt)-Leu-3-methylbutylamide; FRET, fluorescence resonance energy transfer; NFRET, normalized FRET; GFP, green fluorescent protein; MEF, mouse embryonic fibroblast; NLS, nuclear localization signal; YFP, yellow fluorescent protein; DMEM, Dulbecco's modified Eagle's medium.

The aim of our study was to identify proteins interacting with stefin B in the cell nucleus. The fundamental repeating unit of eukaryotic chromatin is the nucleosome, which is composed of an octamer of the four core histones H3, H4, H2A, H2B, around which 147 bp of DNA are wrapped (31). We have shown that stefin B interacts with the histones H2A.Z, H2B, and H3 and with cathepsin L in living cells. In contrast to MENT, we found that nuclear cystatin/stefin B interacted with cathepsin L and with histones in the nucleus, but it did not bind to DNA. Our results suggest that stefin B regulates the activity of cathepsin L in the nucleus and protects the CUX1 transcription factor and probably other substrates from proteolytic cleavage by cathepsin L.

EXPERIMENTAL PROCEDURES

Antibodies—Antibodies to stefin B were described previously (32). Rabbit polyclonal antibody to histone H3 (ab1791), rabbit polyclonal to trimethyl K4 (H3K4me3) (ab8580), and anti-GFP antibody (ab290) were from Abcam. Antibodies to CUX1 (861 and 1300) have been described (13).

Mice—Stefin B (cystatin B)-deficient mice were created as described previously (33). Stefin B-deficient mice were provided by Dr. R. M. Myers, Stanford University, and bred in our local colony. All mice were genotyped by PCR as described previously (33, 34).

Mouse Embryonic Fibroblasts (MEF), Preparation and Cell Cycle Synchronization—MEFs were prepared from individual embryos at embryonic day 14.5. The head and internal organs were removed, and the torso was minced and dispersed in 0.1% trypsin (45–60 min at 37 °C). Cells were grown for two population doublings (considered as one passage) and then viably frozen. MEFs were maintained in DMEM containing 10% fetal bovine serum (Sigma) and subcultured 1:4 on reaching confluence. For serum starvation experiments, MEFs were plated in DMEM containing 0.4% fetal bovine serum and incubated at 37 °C for 72 h before stimulation with DMEM containing 10% fetal bovine serum.

Plasmids and Constructs—The cDNA clone for *CTSB* was obtained from Image (IMAGE, 3453675). It was PCR-amplified and cloned into pcDNA3 vector (Invitrogen) at HindIII and XhoI restriction sites and into pEF/Myc/Nuc vector (Invitrogen), which contains nuclear localization signal and targets the expressed protein to the nucleus at XhoI and BamHI restriction sites. DNA sequence was determined using an ABI PRISM 310 Genetic Analyzer (PerkinElmer Life Sciences). The multiple cloning site of pcDNA3 vector was changed prior to the insertion of T-Sapphire and Venus. This was done in two steps. The first linker, A, was constructed from two oligonucleotides as follows: A, 5′-AAT TCT GCA GGT ATT CTT CAC ACT GGA GGC CGA CCG GGC C-3′, and B, 5′-CGG TCG GCC TCC AGT GTG AAG AAT ACC TGC AG-3′ complementary to A. This was ligated through EcoRI and ApaI restriction sites into pcDNA3 vector. All restriction sites between EcoRI and ApaI in the multiple cloning site of pcDNA3 vector were removed with linker A, among them the restriction site for XhoI and XbaI. Vector pcDNA3 with inserted linker A is labeled pcDNA3L/A. The second linker, B, was constructed from two oligonucleotides as follows: C, 5′-AGC TTC GTC CGC TCG AGA GCG CTT CTA GAG GTC TGG GAG GTT CAG GTG GAG GTG GAG CTG CTG CCG-3′ (XhoI and XbaI sites underlined), and D, 5′-GAT CCG GCA GCT CCA CCT CCA CCT GAA CCT CCC AGA CCT CTA GAA GCG CTC TCG AGC GGA CGA-3′, complementary to C. It was ligated through HindIII and BamHI restriction sites of pcDNA3L/A vector. pcDNA3L/A vector with inserted linker B is labeled pcDNA3L/AB. The cDNAs from Venus YFP (35) and T-Sapphire GFP (36) were amplified by PCR. The resulting products, after BamHI/EcoRI digestion, were cloned into pcDNA3L/AB expression vector. pcDNA3L/AB vector with inserted Venus is labeled Ven-pcDNA3L/AB and with inserted T-Sapphire as T-Sap-pcDNA3L/AB. The cDNA clone for *CTSB* was PCR-amplified, and the resulting product was cloned into T-Sapphire-pcDNA3L/AB after XhoI/XbaI digestion. T-Sap-pcDNA3L/AB construct with inserted stefin B is labeled as Stefin B-GFP. Met-75 cathepsin L was PCR-amplified from procathepsin L cDNA (37), using forward (5′-GCC CGC CTC GAG ATG GCC ATG AAC GCC TTT GG-3′; XhoI site underlined) and reverse (5′-GTC CGC TCT AGA CAC AGT GGC GTA GCT GGC-3′; XbaI site underlined) oligonucleotides. The resulting product, after XhoI/XbaI digestion, was cloned into Venus-pcDNA3L/AB. The Venus-pcDNA3L/AB construct with inserted Met-75 cathepsin L is named M75 cath L-YFP.

Cell Culture—T98G human glioblastoma cell line, ATCC CRL-1690, was from the American Type Culture Collection (Manassas, VA). Cells were cultured as described previously (38). T98G cells were transfected with pEF/Myc/Nuc/stefin B named NB or empty pEF/Myc/Nuc vector alone named NO, using Lipofectamine 2000 (Invitrogen), according to the manufacturer's instructions. Positive clones overexpressing stefin B in the nucleus were obtained after selection with Geneticin (G418) (Invitrogen) (500 μg/ml) and confirmed with Western blots and stefin B-specific enzyme-linked immunosorbent assay (32). CHO-K1 cells (ATCC CCL-61) were cultured in DMEM supplemented with 10% fetal calf serum, 5 units/0.5 ml penicillin, and 5 μg/0.5 ml streptomycin at 37 °C in 5% CO_2. For FRET analysis, cells were seeded at a density of 1×10^5 on glass coverslips and transiently transfected with 1 μg of Stefin B-GFP and 1 μg of M75 cath L-YFP, using Lipofectamine 2000 (Invitrogen), according to the manufacturer's recommendations. The expression of the GFP fusion proteins was determined by Western blot. MCF-7 cells (ATCC HTB-22) were cultured in DMEM supplemented with 10% fetal calf serum, 5 units/0.5 ml of penicillin, and 5 μg/0.5 ml streptomycin at 37 °C in 5% CO_2. Cells were grown on 10-cm Petri dishes, transiently transfected with pEF/Myc/Nuc/stefin B (NB) or empty pEF/Myc/Nuc vector alone (NO), using Lipofectamine 2000 (Invitrogen), according to the manufacturer's instructions. Cells were lysed 24 h post-transfection and nuclear cell lysates prepared as described previously (13).

Preparation of Cell Lysates—Cell lysates were prepared as described previously (34). Nuclear extracts were prepared by the method of Dignam *et al.* (39), with minor modifications, including the use of a protease inhibitor mixture (catalog no. P8340; Sigma) and the addition of phenylmethylsulfonyl fluoride (Fluka, Basel, Switzerland) (0.5 mM) to the resuspension and lysis buffers. Nuclear cell lysates from MCF-7 cells were

prepared as described by Goulet *et al.* (13). In both cases, the supernatants were transferred to fresh test tubes and, if not used immediately, stored at −80 °C. Total protein concentration was determined using the Bradford assay (Bio-Rad).

Co-immunoprecipitation was performed as described previously (34). 5 μg of anti-stefin B polyclonal or monoclonal antibodies (32) were added to nuclear lysates and allowed to rock at 4 °C for 2 h or overnight. 50 μl of protein A-Sepharose beads were then added to the lysates, which were allowed to rock for another hour at 4 °C. Immunoprecipitates were washed three times in cold phosphate-buffered saline. Samples were resolved on SDS-PAGE and analyzed by Western blots.

Western blots were performed as described previously (13, 34). Equal amounts of protein were loaded and resolved in 15, 12.5, or 6% SDS-polyacrylamide gels and electrotransferred to nitrocellulose membranes. Proteins were visualized with ECL (Amersham Biosciences) according to the manufacturer's instructions.

N-terminal Sequencing—Edman sequence analyses of protein samples were performed on a model 492A Procise Protein Sequencing System (Applied Biosystems, Foster City, CA). Proteins were electrotransferred from SDS-polyacrylamide gels to polyvinylidene difluoride membranes and sequenced using a pulsed-liquid blot sequencing protocol. Phenylthiohydantoin-derivatives were analyzed on line on a microbore high pressure liquid chromatography system 140C (Applied Biosystems) using an RP C18 Spheri-5 column (Brownlee). Any cysteine residues were alkylated before sequencing. All reagents and solvents were of sequencing grade (Applied Biosystems).

Cell Cycle Analysis—Cells were trypsinized and pellets fixed in 70% ethanol overnight at −20 °C. After washing, the cells were incubated for 30 min at 37 °C in phosphate-buffered saline containing 40 μg/ml propidium iodide, 100 μg/ml RNase, and 0.05% (w/v) Triton X-100. Finally, cells were washed and resuspended in 0.5 ml of phosphate-buffered saline. Samples were analyzed with a FACSCalibur flow cytometer (BD Biosciences), and cell cycle profiles were evaluated using CellQuest software (BD Biosciences), version 3.3.

FRET Microscopy—FRET measurements were made using a Leica TCS SP5 microscope equipped with a 405-nm laser. The images were acquired with 405- and 515-nm laser lines. Images were taken through a 63 × 1.4-numerical aperture oil immersion objective. To explore the interaction of the Met-75 truncated form of cathepsin L with stefin B, we used a fluorescent protein-protein pair that has excitation and emission properties favorable for FRET; the emission wavelength of T-Sapphire-GFP partially overlaps with the excitation wavelength of YFP (40). For FRET experiments, transient transfections were performed as described above, and expression levels of stefin B-GFP (donor) and Met-75 cathepsin L-YFP (acceptor) proteins were adjusted to similar levels by Western blot. FRET between stefin B-GFP and M75 cath L-YFP was measured in live cells plated on glass-bottomed culture dishes, 18–24 h after transfection. Fluorescence was recorded at three different settings: GFP_{ex}, 405 nm/GFP_{em} 515 nm; YFP_{ex}, 515 nm/YFP_{em}, 523–535 nm; $FRET_{ex}$, 405 nm/$FRET_{em}$, 528–535 nm. Laser power and detector gain were adjusted in the different channels. The image of FRET was generated with the "PixFRET" plug-in for the ImageJ software. In all FRET experiments, negative FRET controls were analyzed after transfection or co-transfection of GFP/YFP or co-transfection R68*X*-GFP/M75 cath L-YFP (negative controls). Bleed through coefficients were calculated using FRET/donor or FRET/acceptor image stacks captured from cells expressing only the donor or acceptor (41). Coefficients were averaged from at least 80 cells from 40 separate stacks for each experiment.

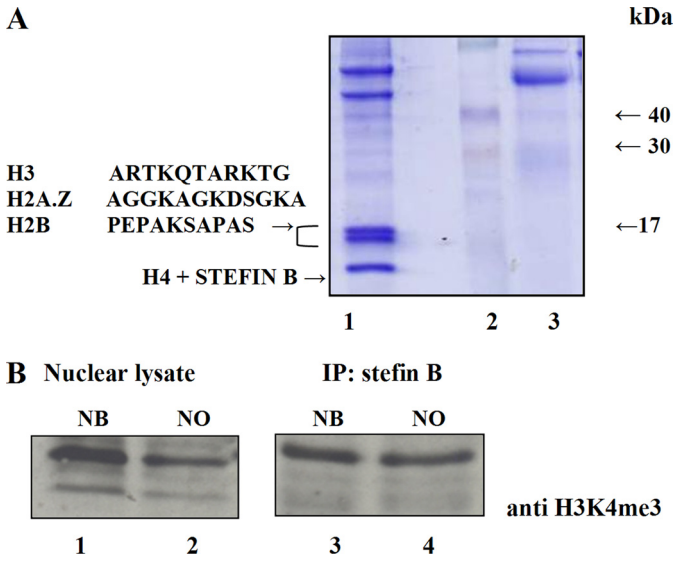

FIGURE 1. **Stefin B in the nucleus co-immunoprecipitates with histones.** *A,* nuclear lysates were prepared as described under "Experimental Procedures" and immunoprecipitated with anti-stefin B antibodies. After SDS-PAGE, gels were stained with Coomassie Blue. The three bands interacting with stefin B were identified as histones by N-terminal amino acid sequencing. N-terminal sequences of the 17- and 14-kDa bands are shown. *Track 1,* nuclear lysates immunoprecipitated with stefin B antibodies; *track 2,* molecular weight standard; *track 3,* control, nuclear lysates immunoprecipitated with antibodies against cathepsin B. *B,* stefin B co-immunoprecipitates with the H3K4me3 histone variant. Nuclear lysates from T98G cells transfected with stefin B in pEF/Myc/Nuc vector (NB) (*track 1*) and control T98G cells transfected with an empty vector pEF/Nuk/Myc alone (NO) (*track 2*) were separated by 15% SDS-PAGE, followed by Western blotting with anti-H3K4me3 antibody. Nuclear lysates from T98G cells transfected with stefin B in pEF/Myc/Nuc vector (NB) (*track 3*) and nuclear lysates from T98G cells transfected with control empty vector (NO) (*track 4*), both immunoprecipitated with stefin B antibodies, were separated by 15% SDS-PAGE, followed by Western blotting with anti-H3K4me3 antibody.

Cathepsin L Inhibition in Vitro—Cathepsin L was preactivated by incubation in 0.1 mM acetate, 1 mM EDTA, 0.1% (w/v) Brij-35, 0.02% (w/v) sodium azide, 10 mM cysteine, pH 5.5, for at least 10 min at room temperature before use. The active enzyme concentration was determined with *trans*-epoxysuccinyl-L-leucylamido-(4-guanidino)-butane (E-64) (Peptide Research Institute, Osaka, Japan) titration. Cathepsin L (final concentration 21.5 nM) was incubated for 5 min with histone isolated from calf thymus (H 4524, Sigma) at final concentrations from 10.8 nM to 2.15 μM. When determining the stefin B and histone interactions, stefin B (final concentration 15 nM) was preincubated with final concentrations of histones from 10.8 nM to 2.15 μM for 5 min, followed by the addition of cathepsin L (final concentration 21.5 nM). After the initial incubation steps, substrate benzyloxycarbonyl-Phe-Arg-*p*-nitroanilide (Bachem, AG, Switzerland) was added to 100 μM

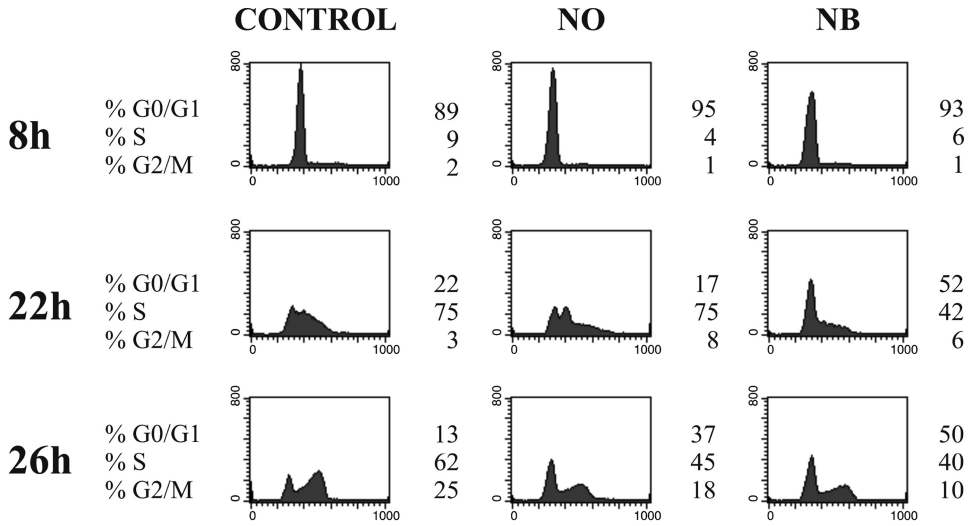

FIGURE 2. **Overexpression of stefin B into the nucleus delays cell cycle progression.** Control T98G cells, T98G cells transfected with an empty vector pEF/Nuk/Myc alone (NO), and T98G cells transfected with stefin B in pEF/Myc/Nuc vector (NB) were harvested at the indicated times, and cell cycle distribution was monitored by flow cytometry analysis after DNA staining with propidium iodide.

final concentration, and initial velocity was determined spectrophotometrically at 410 nM.

RESULTS

Stefin B Interacts with Histones H2A.Z, H2B, and H3 in the Nucleus—With the aim of defining the function of stefin B in the nucleus, we set out to identify proteins that interact with it. Nuclear cell lysates were immunoprecipitated with anti-stefin B antibodies and separated by SDS-PAGE. The 15- and 14-kDa bands were identified as histones H3, H2B, and H2A.Z by N-terminal protein sequencing (Fig. 1*A*). Histone H4 and stefin B were both found around 11 kDa. We found it particularly interesting that stefin B also interacts with the histone H2A.Z variant. The H2A.Z variant is found associated with gene regulatory elements in promoter regions (42). A recent study proposed that H2A.Z is partly co-localized to the same nucleosome as the H3K4me3 histone variant (43). An immunoprecipitation experiment confirmed that the H3K4me3-modified histone also co-immunoprecipitated with stefin B in T98G cells (Fig. 1*B*).

Increased Expression of Stefin B in the Nucleus Delays Cell Cycle Progression—Incubation of cells with the cysteine protease inhibitor E-64d was reported to delay the entry of cells into the S phase of the cell cycle (13, 44). T98G astrocytoma cells were used for cell cycle experiments, as these cells can be synchronized in G_0/G_1 in the absence of serum (38, 45). The effect of E-64d on cell cycle progression was confirmed in synchronized T98G cells (data not shown). Next, we examined whether overexpression of stefin B in the nucleus influences cell cycle progression. T98G cells were transfected with a pEF/Myc/Nuc vector expressing stefin B pEF/Myc/Nuc-stefin B (NB), or an empty vector alone (NO). Expression levels of stefin B in stably transfected T98G cells were quantified by enzyme-linked immunosorbent assay, as described previously (32). In whole cell lysates of cells stably expressing stefin B, the levels of stefin B were 478 ng/mg (ng of stefin B/mg of total cell protein), and in control cells transfected with an empty vector the concentration of stefin B was 178 ng/mg. A marked delay in the progression of cells from the G_1 to the S phase was observed in T98G cells overexpressing stefin B, as compared with control T98G cells and cells transfected with the empty vector alone (NO) (Fig. 2, *22* and *26 h*).

Stefin B Deficiency Leads to Accelerated Entry into S Phase—The influence of stefin B on cell cycle progression was confirmed in MEFs prepared from stefin B-deficient mice and wild type mice. As described previously, the synchronization of MEFs in G_0/G_1 was not as efficient as for T98G cells (46). Nevertheless, cell cycle analysis of synchronized MEFs revealed a small but reproducible acceleration of cell cycle progression from the G_1 to the S phase at 20 and 22 h after serum addition in stefin B-deficient MEFs (Fig. 3). The N-terminally truncated cathepsin L isoform was shown during S phase to localize to the cell nucleus where it cleaves the CUX1 transcription factor (13). The processed isoforms of CUX1 accelerate entry into S phase and stimulate cell proliferation (46). We reasoned that the delay in the cell cycle progression in cells overexpressing stefin B in the nucleus could be attributed to the inhibition of cathepsin L by stefin B.

Increased Expression of Stefin B in the Nucleus Protects CUX1 from Cathepsin L Cleavage—Cathepsin L was shown to cleave CUX1 at multiple sites *in vitro* and *in vivo*, thereby generating a number of processed isoforms collectively called p110 CUX1 (13). Proteolytic processing of CUX1 cannot easily be detected by Western blot analysis in T98G cells.[3] In our experiments, we used MCF-7 cells, which express large amounts of CUX1. MCF-7 cells were transiently transfected with the pEF/Myc/Nuc-stefin B expression vector (NB) or an empty vector (NO), and CUX1 expression was monitored by Western blot analysis. We observed diminished cleavage of full-length CUX1 protein (p200) and diminished p110 fragment formation in cells overexpressing stefin B or treated with the cysteine protease inhibitor E64-d, as compared with cells transfected with an empty vector (NO) (Fig. 4). The reduction in CUX1 cleavage is consistent with the notion that overexpression of stefin B causes the inhibition of cathepsin L in the nucleus.

Visualization of Intracellular Met-75 Cathepsin L-Stefin B Interactions in the Nucleus Using FRET—From structural and kinetics studies that investigated the mechanism of cystatin interaction with papain-like cathepsins, we know that the N-terminal part of cystatins is essential for the interaction with enzymes (47, 48). Therefore, a spectral variant of the GFP-T-Sapphire was fused to the C terminus of stefin B. Venus-YFP was fused to the N- terminal part of the Met-75 human cathepsin L variant. The Met-75-truncated variant of cathepsin L was

[3] A. Nepveu, unpublished data.

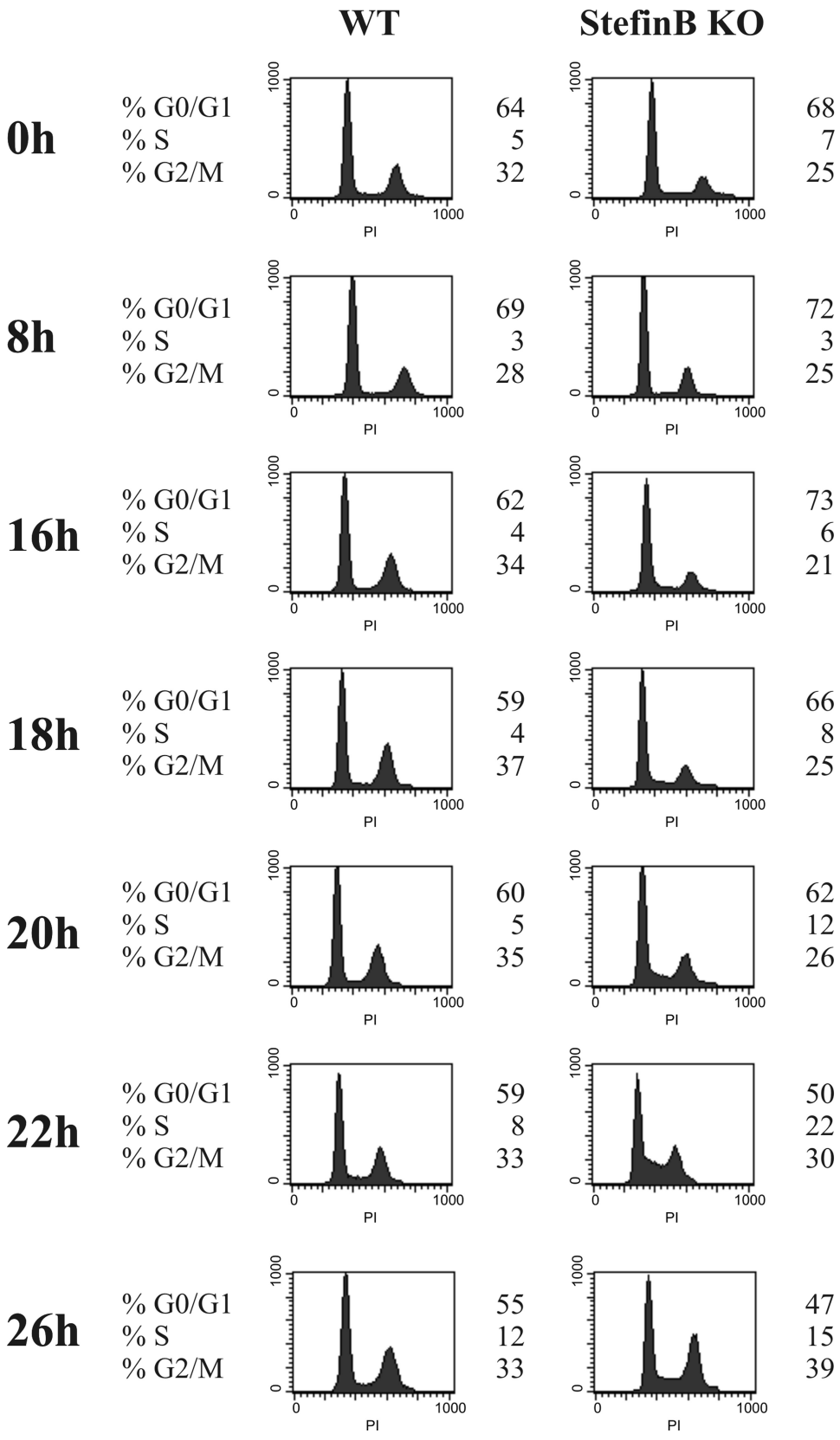

FIGURE 3. **Stefin B deficiency leads to accelerated entry into S phase.** Wild type (*WT*) and stefin B-deficient (*KO*) MEFs were incubated for 72 h in the absence of serum (time point 0). Serum-containing medium was added, and at the indicated time points cell cycle distribution was monitored by flow cytometry analysis after DNA staining with propidium iodide.

found localized in the nucleus (13). In CHO-K1 cells, preferential expression of the Met-75 cathepsin L-YFP fusion protein in the nucleus was observed (Fig. 5*A*). CHO-K1 were chosen for FRET experiments, because they are efficiently transfected (85%) with pcDNA3 expression vector. We used two negative controls as follows: first, a GFP/YFP pair where the two fluorescent proteins are supposed to interact only randomly; second, Met-75 cathepsin L-YFP and a truncated mutant of stefin B, R68*X* (R68Stop), that is found in EPM1 patients and does not inhibit cathepsin L. The biophysical properties of the R68*X* mutant have been studied in detail (49). Spectral bleed through for YFP (acceptor) was 5.2 ± 1.25% and for GFP (donor) was 25.15 ± 0.98%. Images collected in the FRET channel were corrected for donor and acceptor spectral bleed through and normalized for expression levels (NFRET), as described previously (41). NFRET values were measured in the nucleus of 25–30 individual cells for each combination in two separate experiments. Fig. 5*A* provides representative images showing expression of fusion proteins in CHO-K1 cells co-transfected with stefin B-GFP and Met-75 cathepsin L-YFP and control cells co-transfected with R68*X* stefin B-GFP. Normalized FRET (NFRET) values are represented in a gray scale and clearly reveal the existence of FRET in the nuclei of transfected cells but not in control cells transfected with the R68*X* stefin B mutant (Fig. 5*B*). To perform the analysis presented in Fig. 5*B*, the mean values of the intensity, constructed from the NFRET images recorded over the nucleus, were presented as a scatter plot (Fig. 5*C*). When the FRET channel was corrected for the spectral donor (GFP) and acceptor (YFP) bleed through, a NFRET signal in negative control experiments varied between 0 and 20 (Fig. 5*C*). Thus, we have only considered cells with values above a threshold of 20 as positives. In cells transfected with Met-75 cathepsin L-YFP and stefin

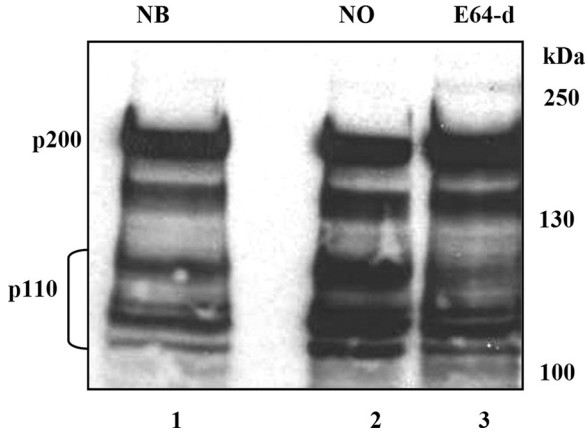

FIGURE 4. **Decreased cleavage of CUX1 transcription factor in MCF-7 cells with increased expression of stefin B in the nucleus.** MCF-7 cells were transfected with pEF/Myc/Nuc-stefin B vector (NB) (*track 1*) in comparison with control cells transfected with pEF/Nuk/Myc alone (NO) (*track 2*) and MCF-7 cells treated with 50 μM E-64d inhibitor (E-64d) (*track 3*).

B-GFP, some of the results were below this threshold (Fig. 5*C*), indicating the possibility that endogenous cathepsin L and stefin B present in the nucleus interacted with GFP fusion proteins and interfered with the results.

Histones Potentiate Inhibition of Cathepsin L by Stefin B—We established that stefin B binds to histones, but the consequences of this interaction are not known. We therefore investigated whether histones influence stefin B inhibitory activity. First, we determined conditions under which inhibition of cathepsin L was in the linear range, *i.e.* up to 70% inhibition. Next, we tested if purified histones inhibit human cathepsin L *in vitro* and found that histones did not inhibit cathepsin L activity even at a 100-fold molar excess (2.15 μM histone concentration) (Fig. 6*A*). To further investigate the role of histones in the inhibition of cathepsin L by stefin B, we preincubated stefin B with increased molar concentrations of histones and measured cathepsin L activity, as described. We found that histone binding to stefin B did not affect the inhibition of cathepsin L by stefin B at lower histone concentrations (10.8–210 nM) (Fig. 6*B*), whereas at higher histone concentrations (1.05–2.15 μM), as found in the nucleus, we observed increased inhibition of cathepsin L by stefin B (Fig. 6*B*).

Stefin B Interacts with Histone H3 in the G_1 Phase of Cell Cycle—The above results led us to examine if the stefin B interaction with histones is cell cycle-dependent. Control T98G cells and T98G cells overexpressing stefin B in the nucleus (NB) were synchronized by serum starvation, as described above. Nuclear lysates were immunoprecipitated with anti-stefin B antibodies, and immunoblotting with anti-H3 antibodies showed that most of the binding of stefin B to histone H3 occurred in the G_1 phase of the cell cycle (Fig. 7). In a control experiment, membranes were immunoblotted with anti-stefin B antibody, confirming the presence of immunoprecipitated stefin B.

Stefin B Does Not Bind DNA—MENT, the serpin that inhibits cathepsin L in the nucleus, is known to bind to histones and DNA, thereby influencing heterochromatin distribution (29, 30). It was demonstrated that the inhibitory activity of MENT on cathepsin L, rather than DNA binding, is crucial for mediating its effect (29). DNA was reported to accelerate the rate at which MENT inhibited cathepsin V, a human ortholog of mammalian cathepsin L, up to 50-fold (50). Therefore, the possible interaction of stefin B with DNA was analyzed by gel shift assay, as described previously (50). However, stefin B did not bind to DNA, in contrast to cathepsin V, which was used as a positive control (Fig. 8). These results therefore suggest that the interaction of stefin B with histones is different from the binding of serpins like MENT, which react with both histones and DNA.

DISCUSSION

Proteolytic activity of cathepsin L in the nucleus has to be under strict control to prevent degradation of transcription factors. Among cystatins, stefin B has been observed in the nucleus, which prompted us to investigate the role of stefin B as a regulator of proteolytic activity of cathepsin L in the nucleus. In this study, we describe for the first time an interaction between a nuclear cystatin, stefin B, and the nucleosomal proteins histone H2A.Z, H2B, and H3 (Fig. 1*A*). The histone H2A.Z variant differs from the canonical H2A in its N-terminal tail sequence and also at key internal residues. This variant has been implicated in several biological processes, such as gene activation, chromosome segregation, heterochromatin silencing, and progression through the cell cycle (51, 52). Histones H2A.Z and H3K4me3 are found at promoter regions, and it has been suggested that these two histone variants partly co-localize to the same nucleosomes (42, 53). A co-immunoprecipitation experiment confirmed that the H3K4me3-modified histone also associates with stefin B in T98G cells (Fig. 1*B*).

In T98G cells in which stefin B was targeted to the nucleus, we have observed a delay in cell cycle progression into S phase (Fig. 2). Increased expression of stefin B into the nucleus resulted in a delay in cell cycle progression comparable with treatments with the synthetic cysteine protease inhibitors E-64d or JPM-OEt (13, 44). Our initial observations were confirmed with the reverse experiment using MEFs from stefin B-deficient mice. Following exit from quiescence, stefin B-deficient MEFs reached the S phase faster than wild type MEFs (Fig. 3). Goulet *et al.* (13) has shown that only shorter procathepsin L isoforms (that start at Met-56, Met-75, Met-77, Met-81, or Met-111) could translocate to the nucleus and stimulate processing of the CUX1 transcription factor at the G_1/S transition of the cell cycle. The processed p110 CUX1 isoform exhibits distinct DNA binding and transcriptional properties: cells overexpressing p110 CUX1 reached the next S phase faster than control cells (13, 46). Therefore, we hypothesized that the cell cycle delay in cells overexpressing stefin B could be attributed to cathepsin L inhibition in the nucleus. Indeed, the steady-state level of p110 CUX1 was reduced in cells overexpressing stefin B, suggesting that cleavage of CUX1 in the nucleus was partially prevented (Fig. 4). Interaction of stefin B with the Met-75 truncated form of cathepsin L in the nucleus was shown by FRET experiments in living cells (Fig. 5, *B* and *C*). This interaction was not entirely unexpected, as *in vitro* kinetic studies have shown that stefin B inhibits cathepsin L with a K_i value in the picomolar range (54, 55). Although increased nuclear localization of procathepsin L in *ras*-transformed mouse fibroblasts was reported more than a decade ago (56), the first physiologically relevant substrates of cathepsin L in the nucleus were

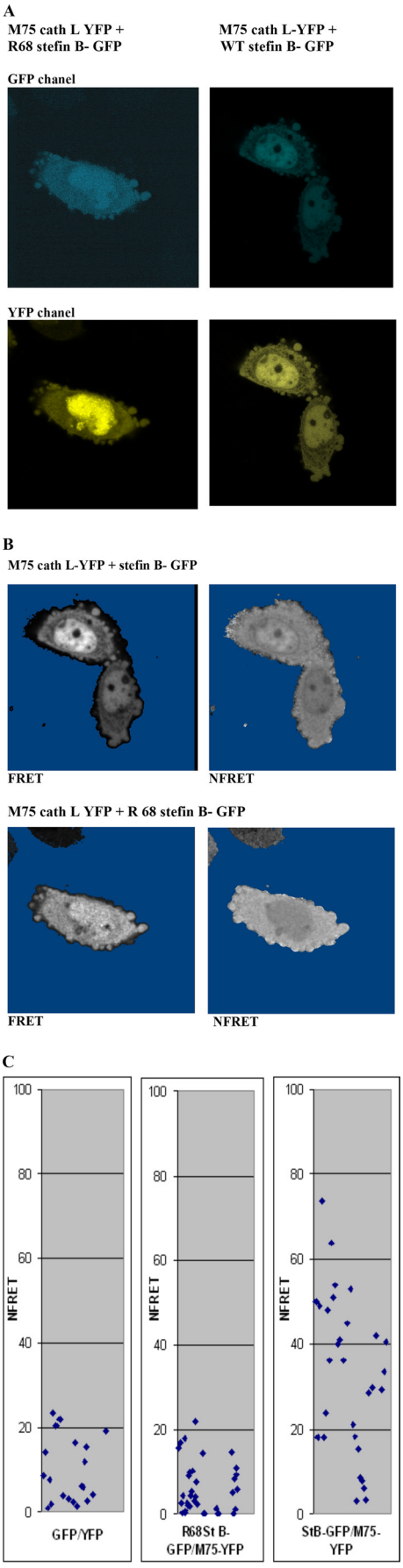

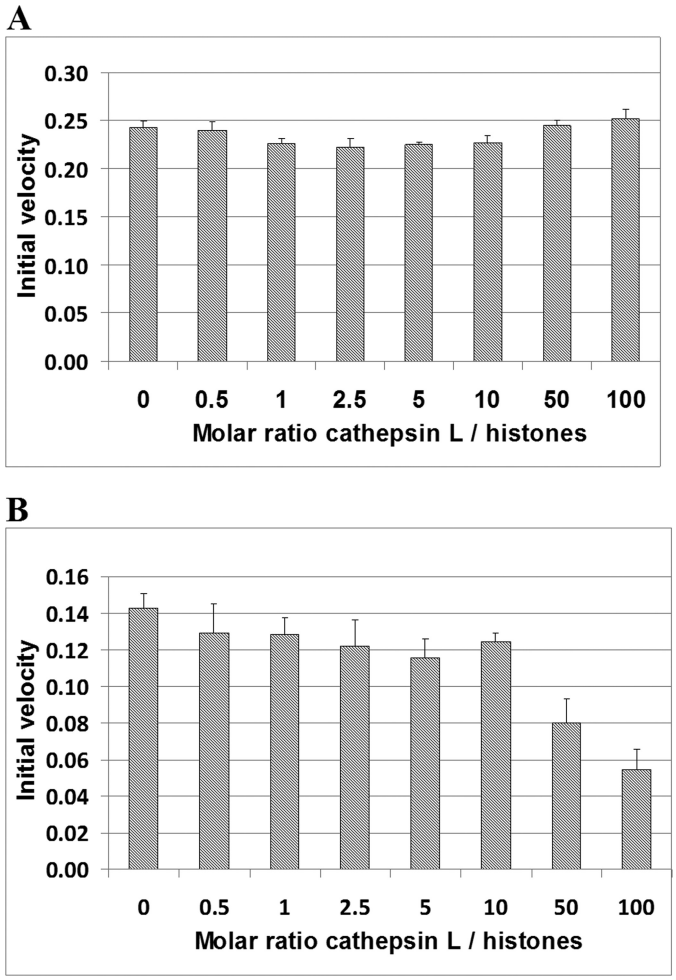

FIGURE 6. **Binding of stefin B to histone increases cathepsin L inhibition by stefin B.** *A,* cathepsin L is not inhibited by histones. Cathepsin L (21.5 nM) was incubated with increasing molar concentrations of histones. The data represent the mean of at least three independent experiments. *B,* addition of histones increased the inhibitory activity of stefin B toward cathepsin L. Stefin B (15 nM) was preincubated with increasing molar concentrations of histones (10.8 nM to 2.15 μM), before the addition of cathepsin L (21.5 nM). The data represent the mean of at least three independent experiments.

described only recently (13, 15, 57). Duncan *et al.* (15) reported that cathepsin L cleaves histone H3 and proposed that this proteolytic activity plays a role in the development and differentiation of mouse embryonic stem cells. We have examined whether the binding of histones to stefin B affects cathepsin L inhibition. *In vitro*, high histone concentrations increased the inhibition of cathepsin L by stefin B. Recently, it was shown that cathepsin L is not the only protease present in the nucleus.

FIGURE 5. **Met-75 cathepsin L and stefin B interact in the nucleus of living cells.** *In situ* analysis of the interaction between stefin B-GFP and Met-75 cathepsin L was measured by FRET. *A,* visualization of Met-75 cathepsin L YFP and Arg-68 stefin B-GFP in CHO K1 cells. The plasmid constructs indicated on *top* of each column were transfected in CHO K1 cells. *B,* visualization of FRET and NFRET in CHO K1 cells pixel-by-pixel analysis of FRET on a cell expressing Met-75 cathepsin L-YFP + stefin B-GFP, performed with the PixFRET plug-in for the ImageJ software. *C,* NFRET in the nuclei of cells transfected with Met-75 cathepsin L YFP + stefin B compared with NFRET in cells transfected with expression vectors for Met-75 cathepsin L/Arg-68 stefin B-GFP. NFRET plot profiles in 25–30 cells were analyzed. Sensitized emission of YFP fusion proteins due to FRET was measured in two separate experiments in the nucleus of 25 individual CHO K1 cells transfected with the indicated combinations of vectors expressing YFP and GFP fusion proteins.

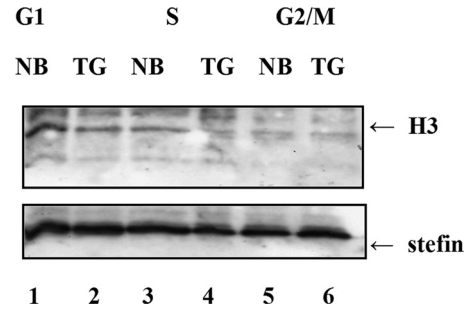

FIGURE 7. **Stefin B interacts with histone H3 predominantly in the G_1 phase of the cell cycle.** T98G cells were synchronized by serum starvation. Nuclear extracts were prepared from T98G cells (*TG*) after 8 h (*G1*), 22 h (*S*), and 26 h (*G2/M*). Protein extracts from T98G cells transfected with stefin B in pEF/Myc/Nuc vector (*NB*) were separated by 15% SDS-PAGE, followed by Western blotting with anti-H3 antibody. Membranes were stripped and immunoblotted with anti-stefin B antibody.

FIGURE 8. **Analysis of stefin B and cathepsin V binding to DNA.** Gel mobility shift analysis of the control protein cathepsin V (*track 1*) and stefin B (*tracks 2–4*) was incubated with ds65-mer DNA. DNA was analyzed by 2% agarose gel electrophoresis. The final concentration (μM) of purified protein in each reaction is indicated at the *top* of each gel panel.

Although it was proposed by Goulet *et al.* (13, 57) that a truncated form of cathepsin F could be active in the nucleus, its nuclear activity was reported only recently. Furthermore, Maubach *et al.* (58) reported that the regulation of nuclear cathepsin F activity by stefin B in hepatic stellate cells was involved in the transcriptional regulation of two activation markers. Together, these findings suggest that the regulatory activity of stefin B in the nucleus may not be limited to its effect on cathepsin L.

MENT, a serpin that also inhibits cathepsins L and V, strongly blocks cell proliferation and promotes condensation of chromatin (29). It was shown that MENT-mediated inactivation of cathepsin L, like cathepsin L deficiency, causes a global rearrangement of chromatin structure and redistribution of specifically modified histones (14, 29). MENT was also reported to interact with DNA (30, 59). Another cysteine protease-inhibiting serpin, SCCA-1 (squamous cell carcinoma antigen-1), has also been shown to localize to the nucleus, but unlike MENT, SCCA-1 is unable to bind to DNA (50). Similarly, we did not observe the binding of stefin B to DNA (Fig. 8). It remains to be tested whether cathepsin inhibitors that do not bind DNA, SCCA-1 and stefin B, have similar effects on heterochromatin redistribution as MENT.

Collectively our results show that stefin B interacts with histones and cathepsin L in the nucleus and regulates cell cycle progression into the S phase. Stefin B was bound to histones preferentially during the G_1 phase of the cell cycle. *In vitro*, high concentrations of histones increased the inhibitory effect of stefin B on cathepsin L activity. Interestingly, entry into S phase is delayed similarly in the presence of the cathepsin L inhibitors E-64d and JPM-OEt or following overexpression of stefin B (Fig. 2) (13, 44).

In addition to the role of stefin B in preventing unwanted cytosolic protease activity resulting from lysosomal leakage, our results demonstrate that stefin B plays an important role in the regulation of cathepsin L proteolytic activity in the nucleus. Stefin B in the nucleus protects cathepsin L substrates from proteolytic processing and consequently participates in transcriptional regulation. It will be interesting to determine whether the loss of cathepsin L inhibition by nonfunctional mutants of stefin B in EPM1 disease is associated with the excessive cleavage of cathepsin L nuclear substrates.

Acknowledgments—The expert technical assistance of Loulou Kroon-Žitko is gratefully acknowledged. We thank Susanne Liebe (Leica Microsystems, Germany) for expert technical help with initial FRET measurements. We thank Roman Jerala (National Institute of Chemistry, Slovenia) for critical reading of the manuscript. We also thank Oliver Griesback (Max-Planck Institute, Germany) for providing plasmid with T-Sapphire GFP and Atsushi Miyawaki (Brain Science Institute, RIKEN, Japan) for plasmid with Venus YFP. We thank. R. M. Myres (Stanford School of Medicine and the Stanford Human Genome Center, Stanford University) for the stefin B-deficient mice.

REFERENCES

1. Turk, V., Turk, B., and Turk, D. (2001) *EMBO J.* **20,** 4629–4633
2. Hsing, L. C., and Rudensky, A. Y. (2005) *Immunol. Rev.* **207,** 229–241
3. Reinheckel, T., Deussing, J., Roth, W., and Peters, C. (2001) *Biol. Chem.* **382,** 735–741
4. Nakagawa, T., Roth, W., Wong, P., Nelson, A., Farr, A., Deussing, J., Villadangos, J. A., Ploegh, H., Peters, C., and Rudensky, A. Y. (1998) *Science* **280,** 450–453
5. Yasothornsrikul, S., Greenbaum, D., Medzihradszky, K. F., Toneff, T.,

Bundey, R., Miller, R., Schilling, B., Petermann, I., Dehnert, J., Logvinova, A., Goldsmith, P., Neveu, J. M., Lane, W. S., Gibson, B., Reinheckel, T., Peters, C., Bogyo, M., and Hook, V. (2003) *Proc. Natl. Acad. Sci. U.S.A.* **100,** 9590–9595
6. Reinheckel, T., Hagemann, S., Dollwet-Mack, S., Martinez, E., Lohmüller, T., Zlatkovic, G., Tobin, D. J., Maas-Szabowski, N., and Peters, C. (2005) *J. Cell Sci.* **118,** 3387–3395
7. Chandran, K., Sullivan, N. J., Felbor, U., Whelan, S. P., and Cunningham, J. M. (2005) *Science* **308,** 1643–1645
8. Simmons, G., Gosalia, D. N., Rennekamp, A. J., Reeves, J. D., Diamond, S. L., and Bates, P. (2005) *Proc. Natl. Acad. Sci. U.S.A.* **102,** 11876–11881
9. Qiu, Z., Hingley, S. T., Simmons, G., Yu, C., Das Sarma, J., Bates, P., and Weiss, S. R. (2006) *J. Virol.* **80,** 5768–5776
10. Puente, X. S., Sánchez, L. M., Overall, C. M., and López-Otín, C. (2003) *Nat. Rev. Genet.* **4,** 544–558
11. Brömme, D., Li, Z., Barnes, M., and Mehler, E. (1999) *Biochemistry* **38,** 2377–2385
12. Santamaría, I., Velasco, G., Cazorla, M., Fueyo, A., Campo, E., and López-Otín, C. (1998) *Cancer Res.* **58,** 1624–1630
13. Goulet, B., Baruch, A., Moon, N. S., Poirier, M., Sansregret, L. L., Erickson, A., Bogyo, M., and Nepveu, A. (2004) *Mol. Cell* **14,** 207–219
14. Bulynko, Y. A., Hsing, L. C., Mason, R. W., Tremethick, D. J., and Grigoryev, S. A. (2006) *Mol. Cell. Biol.* **26,** 4172–4184
15. Duncan, E. M., Muratore-Schroeder, T. L., Cook, R. G., Garcia, B. A., Shabanowitz, J., Hunt, D. F., and Allis, C. D. (2008) *Cell* **135,** 284–294
16. Turk, V., Stoka, V., and Turk, D. (2008) *Front. Biosci.* **13,** 5406–5420
17. Lenarcic, B., and Turk, V. (1999) *J. Biol. Chem.* **274,** 563–566
18. Schick, C., Pemberton, P. A., Shi, G. P., Kamachi, Y., Cataltepe, S., Bartuski, A. J., Gornstein, E. R., Brömme, D., Chapman, H. A., and Silverman, G. A. (1998) *Biochemistry* **37,** 5258–5266
19. Hwang, S. R., Stoka, V., Turk, V., and Hook, V. Y. (2005) *Biochemistry* **44,** 7757–7767
20. Abrahamson, M., Alvarez-Fernandez, M., and Nathanson, C. M. (2003) *Biochem. Soc. Symp.* **70,** 179–199
21. Kopitar-Jerala, N. (2006) *FEBS Lett.* **580,** 6295–6301
22. Riccio, M., Di Giaimo, R., Pianetti, S., Palmieri, P. P., Melli, M., and Santi, S. (2001) *Exp. Cell Res.* **262,** 84–94
23. Lalioti, M. D., Scott, H. S., Buresi, C., Rossier, C., Bottani, A., Morris, M. A., Malafosse, A., and Antonarakis, S. E. (1997) *Nature* **386,** 847–851
24. Lalioti, M. D., Mirotsou, M., Buresi, C., Peitsch, M. C., Rossier, C., Ouazzani, R., Baldy-Moulinier, M., Bottani, A., Malafosse, A., and Antonarakis, S. E. (1997) *Am. J. Hum. Genet.* **60,** 342–351
25. Pennacchio, L. A., Lehesjoki, A. E., Stone, N. E., Willour, V. L., Virtaneva, K., Miao, J., D'Amato, E., Ramirez, L., Faham, M., Koskiniemi, M., Warrington, J. A., Norio, R., de la Chapelle, A., Cox, D. R., and Myers, R. M. (1996) *Science* **271,** 1731–1734
26. Lehesjoki, A. E. (2003) *EMBO J.* **22,** 3473–3478
27. Eldridge, R., Iivanainen, M., Stern, R., Koerber, T., and Wilder, B. J. (1983) *Lancet* **2,** 838–842
28. Alakurtti, K., Weber, E., Rinne, R., Theil, G., de Haan, G. J., Lindhout, D., Salmikangas, P., Saukko, P., Lahtinen, U., and Lehesjoki, A. E. (2005) *Eur. J. Hum. Genet.* **13,** 208–215
29. Grigoryev, S. A., Bednar, J., and Woodcock, C. L. (1999) *J. Biol. Chem.* **274,** 5626–5636
30. Irving, J. A., Shushanov, S. S., Pike, R. N., Popova, E. Y., Brmme, D., Coetzer, T. H., Bottomley, S. P., Boulynko, I. A., Grigoryev, S. A., and Whisstock, J. C. (2002) *J. Biol. Chem.* **277,** 13192–13201
31. Kouzarides, T. (2007) *Cell* **128,** 693–705
32. Kopitar-Jerala, N., Curin-Serbec, V., Jerala, R., Krizaj, I., Gubensek, F., and Turk, V. (1993) *Biochim. Biophys. Acta* **1164,** 75–80
33. Pennacchio, L. A., Bouley, D. M., Higgins, K. M., Scott, M. P., Noebels, J. L., and Myers, R. M. (1998) *Nat. Genet.* **20,** 251–258
34. Kopitar-Jerala, N., Schweiger, A., Myers, R. M., Turk, V., and Turk, B. (2005) *FEBS Lett.* **579,** 2149–2155
35. Nagai, T., Ibata, K., Park, E. S., Kubota, M., Mikoshiba, K., and Miyawaki, A. (2002) *Nat. Biotechnol.* **20,** 87–90
36. Zapata-Hommer, O., and Griesbeck, O. (2003) *BMC Biotechnol.* ***3***, **5**, 1–6
37. Dolinar, M., Maganja, D. B., and Turk, V. (1995) *Biol. Chem. Hoppe-Seyler* **376,** 385–388
38. Stein, G. H. (1979) *J. Cell. Physiol.* **99,** 43–54
39. Dignam, J. D., Lebovitz, R. M., and Roeder, R. G. (1983) *Nucleic Acids Res.* **11,** 1475–1489
40. Zimmermann, T., Rietdorf, J., Girod, A., Georget, V., and Pepperkok, R. (2002) *FEBS Lett.* **531,** 245–249
41. Feige, J. N., Sage, D., Wahli, W., Desvergne, B., and Gelman, L. (2005) *Microsc. Res. Tech.* **68,** 51–58
42. Barski, A., Cuddapah, S., Cui, K., Roh, T. Y., Schones, D. E., Wang, Z., Wei, G., Chepelev, I., and Zhao, K. (2007) *Cell.* **129,** 823–837
43. Schmid, C. D., and Bucher, P. (2007) *Cell* **131,** 831–833
44. Mellgren, R. L. (1997) *Biochem. Biophys. Res. Commun.* **236,** 555–558
45. Hannigan, G., and Williams, B. R. (1986) *EMBO J.* **5,** 1607–1613
46. Sansregret, L., Goulet, B., Harada, R., Wilson, B., Leduy, L., Bertoglio, J., and Nepveu, A. (2006) *Mol. Cell. Biol.* **26,** 2441–2455
47. Machleidt, W., Thiele, U., Laber, B., Assfalg-Machleidt, I., Esterl, A., Wiegand, G., Kos, J., Turk, V., and Bode, W. (1989) *FEBS Lett.* **243,** 234–238
48. Stubbs, M. T., Laber, B., Bode, W., Huber, R., Jerala, R., Lenarcic, B., and Turk, V. (1990) *EMBO J.* **9,** 1939–1947
49. Rabzelj, S., Turk, V., and Zerovnik, E. (2005) *Protein Sci.* **14,** 2713–2722
50. Ong, P. C., McGowan, S., Pearce, M. C., Irving, J. A., Kan, W. T., Grigoryev, S. A., Turk, B., Silverman, G. A., Brix, K., Bottomley, S. P., Whisstock, J. C., and Pike, R. N. (2007) *J. Biol. Chem.* **282,** 36980–36986
51. Dhillon, N., Oki, M., Szyjka, S. J., Aparicio, O. M., and Kamakaka, R. T. (2006) *Mol. Cell. Biol.* **26,** 489–501
52. Jin, C., and Felsenfeld, G. (2007) *Genes Dev.* **21,** 1519–1529
53. Schones, D. E., Cui, K., Cuddapah, S., Roh, T. Y., Barski, A., Wang, Z., Wei, G., and Zhao, K. (2008) *Cell* **132,** 887–898
54. Kastelic, L., Turk, B., Kopitar-Jerala, N., Stolfa, A., Rainer, S., Turk, V., and Lah, T. T. (1994) *Cancer Lett.* **82,** 81–88
55. Pol, E., and Björk, I. (2003) *Biochim. Biophys. Acta* **1645,** 105–112
56. Hiwasa, T., and Sakiyama, S. (1996) *Cancer Lett.* **99,** 87–91
57. Goulet, B., Sansregret, L., Leduy, L., Bogyo, M., Weber, E., Chauhan, S. S., and Nepveu, A. (2007) *Mol. Cancer Res.* **5,** 899–907
58. Maubach, G., Lim, M. C., and Zhuo, L. (2008) *Mol. Biol. Cell* **19,** 4238–4248
59. Istomina, N. E., Shushanov, S. S., Springhetti, E. M., Karpov, V. L., Krasheninnikov, I. A., Stevens, K., Zaret, K. S., Singh, P. B., and Grigoryev, S. A. (2003) *Mol. Cell. Biol.* **23,** 6455–6468